NANO LETTERS

2008
Vol. 8, No. 10
3205-3210

Self-Assembled Shape- and Orientation-Controlled Synthesis of Nanoscale Cu_3Si Triangles, Squares, and Wires

Zhou Zhang,[†] Lai Mun Wong,[||] Hock Guan Ong,[§] Xin Jiao Wang,[‡] Jun Ling Wang,[§] Shi Jie Wang,[||] Hongyu Chen,[*,‡] and Tom Wu[*,†]

Division of Physics and Applied Physics, Division of Chemistry and Biological Chemistry, School of Physical and Mathematical Sciences, Nanyang Technological University, Singapore 637371, Singapore, School of Materials Science and Engineering, Nanyang Technological University, Singapore 639798, Singapore, and Institute of Materials Research and Engineering, 3 Research Link, Singapore 117602, Singapore

Received May 28, 2008; Revised Manuscript Received August 3, 2008

ABSTRACT

Controlling shape and orientation is important for the synthesis of functional nanomaterials. In this work, nanoscale Cu_3Si triangles, squares, and wires have been grown on Si(111), (100), and (110) substrates, respectively, through a template-free Au-nanoparticle-assisted vapor transport method. The sides of nanotriangles and nanosquares and the growth direction of the nanowires are all along Si ⟨110⟩, giving rise to long-range ordering of the nanostructures. Au nanoparticles absorb Cu vapor and facilitate the rate-limited diffusion of Si, which is critical for the shape-controlled growth of Cu_3Si. This bottom-up approach to synthesize shape- and orientation-controlled Cu_3Si nanostructures might be applicable to the tailored growth of other materials.

Understanding the silicon/metal interactions and the resulting silicides are important for both fundamental sciences and semiconductor technologies. One main theme in studying metal silicides is to search for high-performance interconnects, ohmic contact, and gate materials for electronic circuitry.[1] As the dramatic shrinking of transistors continues, metallic silicide nanowires (NW) of TiSi, CoSi, NiSi, Ni_2Si, TaSi, and PtSi were envisioned to be natural building blocks for semiconductor devices.[2−6] Recently, a lot of attentions and activities also fall on FeSi, CoSi, $Fe_{1-x}Co_xSi$, and Fe_5Si_3 NWs due to their potential applications in silicon-based spintronics.[7,8] Besides these electronic applications, $CrSi_2$ NWs were synthesized and explored as thermoelectric materials for energy generation.[9,10]

To construct nanoscale silicides, self-assembly is an effective bottom-up approach to overcome the limitations on resolution and throughput of the conventional lithographic techniques.[11] Previously, free-standing NWs were grown by chemical vapor transport from metal halides[6,7,9] or single-source organometallic precursors.[4,12] Growth of silicide NWs was also achieved by annealing metal or silicide films under controlled embients.[5] In addition to free-standing NWs, straight silicide NWs attached to silicon wafers were fabricated based on asymmetric lattice mismatches between the silicides and the host silicon substrates. With the silicon substrates acting as templates, self-assembled epitaxial growths of silicide NWs on Si substrates have been demonstrated.[2,13] Silicide NWs can also grow without anisotropic lattice mismatch, following the endotaxial or the strain-driven "shape transition" mechanism.[14]

So far, there has been no report on the controlled synthesis of Cu_3Si nanostructures although the Cu/Si interface, and the formation of copper silicides were thoroughly investigated due to their microelectronic and catalytical applications.[15−21] Furthermore, there is a lack of shape-controlled synthesis of silicide nanostructures; besides nanowire, nanodot was among the few types of

* To whom correspondence should be addressed. E-mail: (T.W.) tomwu@ntu.edu.sg; (H.Y.C.) hongyuchen@ntu.edu.sg.

† Division of Physics and Applied Physics, Nanyang Technological University.

‡ Division of Chemistry and Biological Chemistry, School of Physical and Mathematical Sciences, Nanyang Technological University.

§ School of Materials Science and Engineering, Nanyang Technological University.

|| Institute of Materials Research and Engineering.

10.1021/nl8015208 CCC: $40.75
Published on Web 09/03/2008

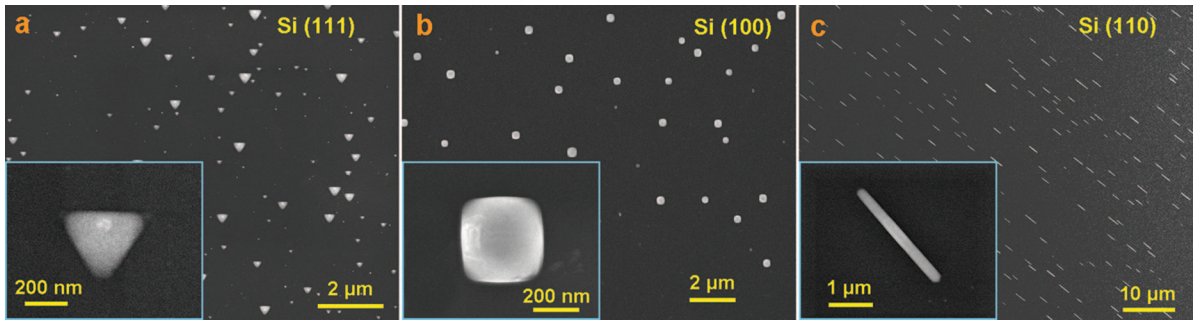

Figure 1. SEM images of shape-controlled Cu_3Si nanostructures grown at 960 °C for 1 min using 30 nm Au NPs as catalyst. NTs, NS, and NWs are synthesized on substrates of (a) Si(111), (b) Si(100), and (c) Si(110), respectively. Insets show magnified views of individual nanostructures.

morphologies reported.[22] For functional materials like silicides, tailoring the morphologies of nanostructures is important for achieving the desired physical and chemical properties.[23,24] In this work, long-range ordered Cu_3Si nanotriangles (NTs), nanosquares (NSs), and NWs were synthesized on Si (111), (100), and (110) surfaces, respectively, by using a chemical vapor transport method. Different from most of the previous studies, Au nanoparticles (NPs) were used as catalyst to effectively absorb the Cu vapor and to penetrate the native SiO_2 layer, facilitating the Cu−Si reaction. This facile method of shape-controlled nanoscale growth does not require a UHV environment and might be applicable for the synthesis of other nanomaterials.

The growth of Cu_3Si nanostructures was carried out in a home-built system comprised of a quartz tube heated by a horizontal tube furnace (Supporting Information I and Figure S1).[25] Si substrates with (111), (110), or (100) orientations were cleaned before Au NPs were dispersed on the surfaces. Mixed powder of CuO and graphite with a total weight of 0.1 g and a weight ratio of 1:1 was used as the source of Cu vapor. Ar was introduced as the carrying gas with a constant flow rate of 50 sccm and the pressure inside the quartz tube was maintained at 20 mbar. During the growth, the source and the substrate temperatures were calibrated to be 960 and 850 °C, respectively. The furnace tube was heated for a predetermined period of time and then quickly cooled down to room temperature. A scanning electron microscope (SEM) and a high-resolution transmission electron microscope (HRTEM) were used to study the sample morphology and structure. The composition was determined by X-ray diffraction (XRD) and energy-dispersive X-ray spectroscopy (EDX).

Figure 1 shows representative SEM images of the samples after growth of 1 min. The substrate orientation and symmetry dictate the shape of the nanostructures. Nanoscale triangles, squares, and wires were observed on Si (111), (100), and (110) substrates, respectively. The equilateral NTs and NSs exhibit lateral dimensions from 140 to 350 nm, and from 240 to 380 nm, respectively. NWs have width between 190 and 390 nm, and length between 0.6 and 6.2 μm. In a given sample, all the nanostructures have the same orientation. The boundaries of NTs and NSs and the growth direction of the NWs were determined to be along the Si ⟨110⟩ directions (Supporting Information, Figure S2). As depicted in the insets of Figure 1, the corners of the NTs, NSs, and NWs are always rounded, the tops not flat.

Thirty nanometer Au NPs were used as catalyst in the experiments, and in the inset of Figure 1a a Au NP can be identified inside the NT. Au NPs were found to be crucial for the growth of Cu_3Si nanostructures; control experiments not using Au NPs did not give any product with regular shape. Careful examinations, however, indicate that only a small fraction (~5%) of the Au NPs eventually led to the growth of nanostructures (Supporting Information, Figure S3), and the process of selective nucleation appears to be subtle.

To characterize the chemical compositions of the nanostructures, XRD studies were carried out. As shown in Figure 2a, the XRD peaks located at 36.5, 42.3, 44.6, and 45.2° indicate an η-Cu_3Si structure for all three samples. Although the XRD peaks are weak due to the low surface coverage of Cu_3Si, they indicate that the nanostructures are at least partially crystalline, not amorphous. The week peak at 38.3° can be assigned to either Au or Cu−Au alloy. According to the Cu−Si binary phase diagram,[26] η-Cu_3Si comprises three phases which appear at different temperature zones and are denoted as η, η', and η''. During the cooling process following the high-temperature synthesis, a phase transformation of $\eta \rightarrow \eta' \rightarrow \eta''$ occurrs.[15] η'' is the equilibrium phase at room temperature, and its structure can be considered as a disordered η' superstructure with periodic displacements normal to the η' [111] direction.[15] Figure 2b illustrates the crystal structure of η'-Cu_3Si and the atoms in Cu_3Si are located at similar positions as Si atoms in a Si unit cell. The XRD peaks and the Cu_3Si planes in Figure 2 are indexed as the η' phase (rhombohedric, S.G. $R\bar{3}$, a = 4.72 Å, α = 95.72°, Supporting Information II).[15]

Compared with the powder counterpart (JCPDS Card No. 51-0916), the η' (111) peak is significantly enhanced in all the samples examined, suggesting a preferred growth along the [111] direction. For Cu_3Si NTs grown on Si (111), η' (111) plane may establish epitaxy with Si (111) as illustrated in Figure 2b. For Cu_3Si NSs grown on Si (100), on the other hand the enhanced η' (111) diffraction implies a polycrystalline nature in accord with the previous observation of pyramidal pits with {111} Cu_3Si side surfaces formed on Si (100).[21] Overall, the shapes of Cu_3Si nanostructures are well defined by the orientations of the Si substrates, although the Cu_3Si nanostructures may not

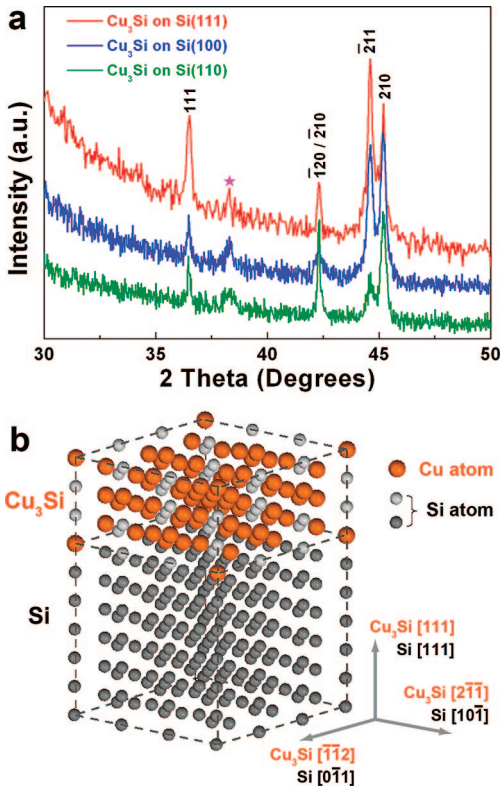

Figure 2. (a) XRD data of Cu_3Si nanostructures grown on Si (111), (100), and (110) substrates. The peak marked with star can be assigned to Au or Cu−Au alloy. (b) Schematic illustration of η'-Cu_3Si crystal structure on Si (111).

be single crystals. As we will show later, an oxide layer was observed at the Cu_3Si/Si interface, which excludes a complete epitaxial growth. The top surfaces of nanostructures roughen further as the growth continues, indicating the formation of polycrystalline precipitates (Supporting Information, Figure S4). Nevertheless, both the XRD data and the shape-controlled growth imply a partially crystalline nature of the Cu_3Si nanostructures, which is consistent with the previous reports on Cu_3Si precipitates in Si.[15]

Spatially correlated SEM imaging and EDX mapping confirmed the Cu_3Si phase in the nanostructures as detected by XRD. To achieve better image quality, large-size structures obtained by extending the growth time from 1 to 15 min (Figure 3) were chosen. The self-assembled structures are Cu rich; but the exact mole ratio between Cu and Si can not be unambiguously determined due to the contribution of Si signal from the substrates.

Cross-section TEM imaging and EDX analysis were used to study the Cu_3Si/Si interface and the growth mechanism. Several Cu_3Si NT samples were grown for 1 min with 15 nm Au NPs and were thinned for TEM observation. For the EDX analysis, Mo TEM grids were used in order to eliminate the Cu signal from the commonly used Cu grids. The cross-section image in Figure 4a suggests that an Au NP is buried inside the Cu_3Si NT. Silicon under the Cu_3Si NT is partly "etched" and forms a valleylike morphology, which is similar to the endotaxy growth.[20] In line with the previous studies, the Si substrate appears to be consumed as a source of Si atoms in the Cu_3Si reaction. Because of its polycrystalline

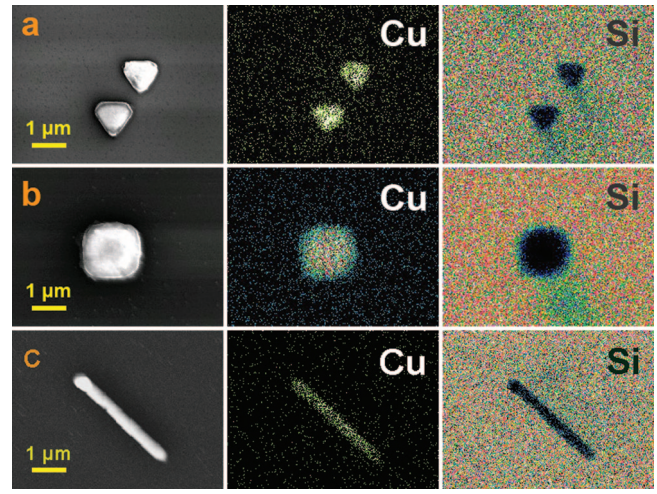

Figure 3. SEM images of Cu_3Si nanostructures and EDX element mappings of Cu and Si for (1) NT on Si (111), (b) NS on Si (100), and (c) NW on Si (110).

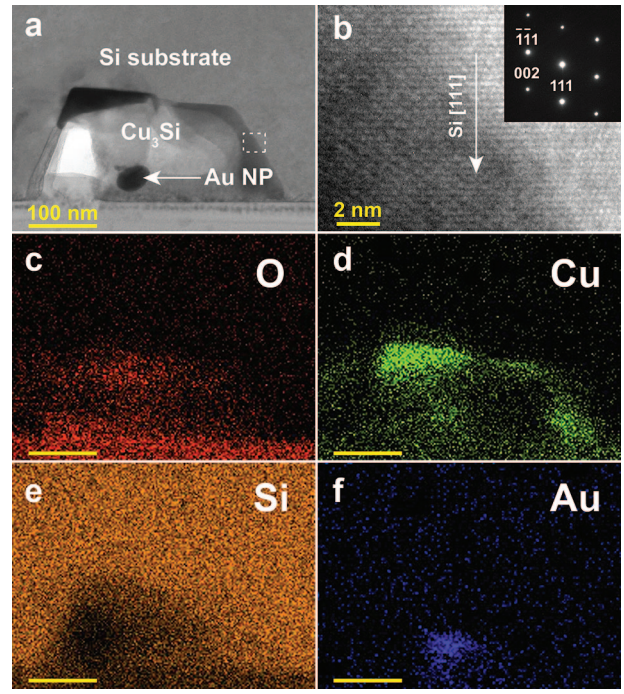

Figure 4. Cross-section TEM and EDX data of a Cu_3Si NT on Si (111) substrate. (a) Cross-section TEM image. (b) HRTEM image and SEAD pattern corresponding to panel a. (c−f) EDX mappings of elements O, Cu, Si, and Au.

nature, Cu_3Si is more fragile than the single crystalline Si and Au. Since the sample preparation process involves dimpling and ion-mill thinning, special cares were taken to avoid sample amorphization. HRTEM image in Figure 4b shows lattice fringes of Cu_3Si, and the selected area electron diffraction (SEAD) pattern indicates a crystalline nature.

EDX element mapping of O, Cu, Si, and Au were carried out (Figure 4c−f). Figure 4d,f suggests that the Au NP is also rich in Cu, which reflects their important role in absorbing and supplying Cu for the silicide reaction. According to the Au−Cu binary phase diagram, Au is very effective to accommodate Cu.[26] At the high growth temperature, the liquidized surface of Au NPs effectively absorbs

the Cu vapor. In the control experiments, no silicide was observed in the absence of Au NP, which is analogous to the vapor−liquid−solid growth of semiconductor NWs.[27] The formation of the oxide layer in Figure 4c, as defined by the higher oxygen intensity, is quite intriguing. Although there is always a native SiO_2 layer on silicon wafer, it may not be the only source contributing to this oxide region. Si atoms in Cu_3Si are more active than those in pure Si in a wide range of temperature, and they are readily oxidized when exposed to air.[18] Therefore, the oxide layer might be quite thin in the as-grown samples synthesized in an oxygen-poor environment. However, it possibly thickened during the TEM sample preparation process comprising polishing, thinning, and air exposure. Near the Cu_3Si/Si interface, the oxidization product should be SiO_2 instead of CuO or CuO_2 because the bonding energy of Si−O is larger than that of Cu−O.[28] This is consistent with the XRD result that no CuO or CuO_2 peaks were found in Cu_3Si samples.

Besides absorbing Cu vapor, Au NPs may play another crucial role in penetrating the oxide barrier, which makes the Cu/Si reaction possible. It is known that Cu_3Si is the thermo-equilibrium phase and forms at the Cu−Si interface even at low temperatures. However, even a SiO_2 layer of only a few nanometers can block the diffusion of both Si and Cu, thus preventing the formation of silicides.[19] In all previous reports using Si substrates as growth templates, the native oxide layer on Si must be carefully removed and the experiments were carried out in a UHV environment to minimize oxidation. In contrast, in our experiments, the AuNPs facilitated the Cu_3Si formation even in the presence of a SiO_2 barrier. A eutectic temperature of mere 363 °C allows Au and Si to form alloys.[26] At high growth temperatures (>450 °C), Au NPs likely react with silicon, and this reaction may force oxygen to diffuse deeper into the substrate or to release into vacuum, which effectively destroys the oxide layer.[29,30] Concurrently, as the cross-section EDX mappings indicates, Au also adsorbs copper vapor to form liquid alloy. Therefore, in our experiments, the Au NPs play two roles: one is to absorb the Cu vapor and another is to help Si and Cu to mix and react through the blocking barrier of SiO_2 by forming alloys with both elements. In Figure 4d,e, the higher concentrations of Cu and Si in and around the Au NP also support our hypothesis of Au catalyst-assisted growth of Cu_3Si. After the initial formation of a crystalline template layer, the silicide reaction is further limited by the diffusion of Si through the established silicide layer. The rate of diffusion is strongly temperature dependent, which explains the fact that a good shape control was achieved only at growth temperatures higher than 800 °C (Supporting Information, Figure S5). The shape control diminished at lower temperatures and totally disappeared at 700 °C.

Additional control experiments were carried out to elucidate the critical roles the Au NPs play in the synthesis of nanoscale Cu_3Si. We investigated the interaction between the Au NPs and the Si substrates and the origin of the low yield of silicide nanostructures. Si substrates were coated with Au NPs and annealed at 960 °C in Ar. As expected, the high mobility at the annealing temperature caused Au NPs to migrate and coalesce through an Ostwald ripening process, which dramatically decreased the total number of NPs as well as the resulting Cu_3Si nanostructure. After annealing, Au was chemically etched, and tiny holes were observed (Supporting Information, Figure S6), which indicates that Au NPs are capable to penetrate the SiO_2 layer and form alloys with Si. In addition, we evaluated the ability of Au NPs to penetrate through the native oxide layer on the Si substrate. The diffusion of Au and Si and the reduction of SiO_2 are hindered if the oxide layer is too thick.[30] Si (111) substrates with different oxide thicknesses (5, 10, 20, 50, and 100 nm) were prepared and used for the silicide growth. The formation of Cu_3Si NTs was terminated when the SiO_2 layer is thicker than 50 nm (Supporting Information, Figure S7), which suggests that the diffusion through the SiO_2 layer is a limiting factor in the silicide growth.

The substrate-dictated alignment of the NTs is consistent with the previous reports on Cu_3Si islands grown on Si (111) surface.[17,20] When 100 monolayers of Cu were deposited on Si (111) in a high-temperature UHV environment, 3D silicide islands were observed following the growth of a 2D layer. The coexistence of multiple crystallographic growth habits led to the formation of polyhedral, triangular, irregular-hexagonal, and rod-shaped crystallites.[17,20] On the other hand, in our experiments on Si (111) the transport of Cu vapor brought about the formation of only NTs, which contrasts with the previous reports. Furthermore, the formation of the thin-film-supported silicide islands in the previous studies required an oxygen-free UHV environment; the growth was significantly retarded by a thin layer of native oxide on Si.[19] In the current work, the remarkable shape control and the alignment along the close-packed Si directions resonate with the quantum growth of metal nanoplatelets.[31]

The orientation of the silicon substrates controls the shape of the Cu_3Si nanostructures; in addition, two other parameters, namely, the Au NP size and the heating time affect their sizes. Au NPs with diameters of 4.8 ± 1.2, 13.5 ± 1.0, and 37.0 ± 2.0 nm were used and the heating duration at 960 °C was varied from 0 to 3 min. The growth started before the temperature reached 960 °C and Cu_3Si nanostructures were observed in all the experiments. The dimensions of more than 400 Cu_3Si nanostructures were measured for each sample, and the results are shown in Figure 5 and Supporting Information, Table S1. Generally speaking, the nanostructure sizes increase with larger Au NP diameters or longer growth times, which offers additional controls on the synthesis. With larger Au NPs, the length of the NWs reaches tens of μm, while the width remains around 500 nm.

When the growth time exceeds 30 min, flowerlike fractal patterns appear on triangle and square surfaces, and the nanowire surfaces become very rough (Supporting Information, Figure S8). Similar to the nanostructures, the large-size polycrystalline precipitates appear to be Cu_3Si (Supporting Information, Figure S4). The formation of such branched fractal patterns indicates a nonequilibrium growth with oscillatory nucleation.[24] The small size of Au NPs and their localized absorption of Cu vapor may also cause nonuniform growth of polycrystalline products; this tendency

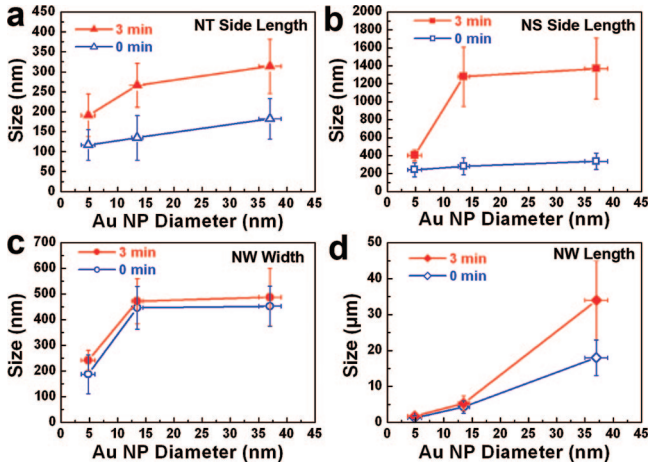

Figure 5. Size control of the Cu_3Si nanostructures by adjusting Au NP diameter and growth time at 960 °C.

become more pronounced when the Cu_3Si structures grow larger. Furthermore, the phase change during cooling may cause nonuniform distribution of strains and contribute to the structural distortion and the formation of polycrystalline structures. When the size of the triangle exceeds 3 μm, the surface roughening is quite significant; its boundary, however, remains well defined. This robust shape control might be a result of the strong orientation dependence of the diffusion of Si atoms, in line with our proposed growth mechanism.

In summary, Cu_3Si nanostructures with long-range ordering and shape control have been synthesized through a facile vapor transport method. Nanotriangles, nanosquares, and nanowires were obtained on Si (111), (100), and (110) substrates, respectively. A diffusion limited growth mechanism was proposed, where Au NP play crucial catalytic roles not only in absorbing the Cu vapor but also in facilitating the Cu/Si diffusion. Additional size control of the nanostructures was achieved by tuning Au NP diameter and growth time. More efforts are needed to achieve higher yield and uniform size. Furthermore, the electrical and catalytical properties of these Cu_3Si nanostructures need to be characterized (Supporting Information III and Figure S9). Our preliminary results suggest that cobalt silicide NTs can also be grown on Si (111) although the control is not as good as in Cu_3Si (Supporting Information IV and Figure S10). This versatile pathway to fabricate nanostructures with controlled shape and order may assist the designed synthesis and assembly of nanostructures in other material systems and help reveal novel properties and applications.

Acknowledgment. T.W. thanks NTU (SUG 20/06), MOE (RG 46/07), and IMRE for support. H.Y.C. acknowledges MOE (ARC 27/07). T.W. also thanks Dr. Paul Mertens for helpful discussion.

Supporting Information Available: Equipment setup and experimental details; further discussion on the crystal structure of Cu_3Si; additional SEM images and EDX data of Cu_3Si NTs, NSs and NWs; interaction between Au NPs and silicon substrate; effect of the SiO_2 layer on the formation of Cu_3Si NTs; effects of growth temperature and growth time on the growth of Cu_3Si nanostructures; preliminary electrical characterization of NTs; growth of cobalt silicide NTs on Si (111); a table illustrating the effects of Au NPs and growth time on the size of the Cu_3Si nanostructures. This material is available free of charge via the Internet at http://pubs.acs.org.

References

(1) (a) Murarka,; S. P. *Silicides for VLSI Application*; Academic: New York, 1983. (b) Zhang, S. L.; Ostling, M. *Crit. Rev. Solid State Mater. Sci.* **2003**, *28*, 1. (c) Chen, L. J. *JOM* **2005**, *57*, 24–30.
(2) (a) Hsu, H. C.; Wu, W. W.; Hsu, H. F.; Chen, L. J. *Nano Lett.* **2007**, *7*, 885–889. (b) Lim, D. K.; Lee, D.; Lee, H.; Bae, S. S.; Choi, J.; Kim, S.; Ji, C. X.; Ragan, R.; Ohlberg, D. A. A.; Chang, Y. A.; Williams, R. S. *Nanotechnology* **2007**, *18*, 095706.
(3) (a) Okino, H.; Matsuda, I.; Hobara, R.; Hosomura, Y.; Hasegawa, S.; Bennett, P. A. *Appl. Phys. Lett.* **2005**, *86*, 233108. (b) Wu, Y.; Xiang, J.; Yang, C.; Lu, W.; Lieber, C. M. *Nature* **2004**, *430*, 61. (c) Liu, B. Z.; Wang, Y. F.; Dilts, S.; Mayer, T. S.; Mohney, S. E. *Nano Lett.* **2007**, *7*, 818. (d) Lin, Y. C.; Lu, K. C.; Wu, W. W.; Bai, J. W.; Chen, L. J.; Tu, K. N.; Huang, Y. *Nano Lett.* **2008**, *8*, 913–918.
(4) Schmitt, A. L.; Zhu, L.; Schmeisser, D.; Himpsel, F. J.; Jin, S. *J. Phys. Chem. B* **2006**, *110*, 18142–18146.
(5) (a) Decker, C. A.; Solanki, R.; Freeouf, J. L.; Carruthers, J. R.; Evans, D. R. *Appl. Phys. Lett.* **2004**, *84*, 1389–1391. (b) Kim, C. J.; Kang, K.; Woo, Y. S.; Ryu, K. G.; Moon, H.; Kim, J. M.; Zang, D. S.; Jo, M. H. *Adv. Mater.* **2007**, *19*, 3637. (c) Chueh, Y. L.; Chou, L. J.; Cheng, S. L.; Chen, L. J.; Tsai, C. J.; Hsu, C. M.; Kung, S. C. *Appl. Phys. Lett.* **2005**, *87*, 223113. (d) Chueh, Y. L.; Ko, M. T.; Chou, L. J.; Chen, L. J.; Wu, C. S.; Chen, C. D. *Nano Lett.* **2006**, *6*, 1637–1644.
(6) Song, Y. P.; Schmitt, A. L.; Jin, S. *Nano Lett.* **2007**, *7*, 965–969.
(7) (a) Ouyang, L.; Thrall, E. S.; Deshmukh, M. M.; Park, H. *Adv. Mater.* **2006**, *18*, 1437. (b) Seo, K.; Varadwaj, K. S. K.; Mohanty, P.; Lee, S.; Jo, Y.; Jung, M. H.; Kim, J.; Kim, B. *Nano Lett.* **2007**, *7*, 1240–1245. (c) Varadwaj, K. S. K.; Seo, K.; In, J.; Mohanty, P.; Park, J.; Kim, B. *J. Am. Chem. Soc.* **2007**, *129*, 8594–8599.
(8) Schmitt, A. L.; Higgins, J. M.; Jin, S. *Nano Lett.* **2008**, *8*, 810–815.
(9) (a) Seo, K.; Varadwaj, K. S. K.; Cha, D.; In, J.; Kim, J.; Park, J.; Kim, B. *J. Phys. Chem. C* **2007**, *111*, 9072–9076. (b) Szczech, J. R.; Schmitt, A. L.; Bierman, M. J.; Jin, S. *Chem. Mater.* **2007**, *19*, 3238–3243.
(10) Zhou, F.; Szczech, J.; Pettes, M. T.; Moore, A. L.; Jin, S.; Shi, L. *Nano Lett.* **2007**, *7*, 1649–1654.
(11) (a) Tai, K. L.; Vadimsky, R. G.; Kemmerer, C. T.; Wagner, J. S.; Lamberti, V. E.; Timko, A. G. *J. Vac. Sci. Technol.* **1980**, *17*, 1169–1176. (b) Howard, R. E.; Hu, E. L.; Jackel, L. D.; Grabbe, P.; Tennant, D. M. *Appl. Phys. Lett.* **1980**, *36*, 592–594.
(12) Schmitt, A. L.; Bierman, M. J.; Schmeisser, D.; Himpsel, F. J.; Jin, S. *Nano Lett.* **2006**, *6*, 1617–1621.
(13) (a) Chen, Y.; Ohlberg, D. A. A.; Medeiros-Ribeiro, G.; Chang, Y. A.; Williams, R. S. *Appl. Phys. Lett.* **2000**, *76*, 4004–4006. (b) Carter, J. D.; Cheng, G. J.; Guo, T. *J. Phys. Chem. B* **2004**, *108*, 6901–6904. (c) Zou, Z. Q.; Wang, H.; Wang, D.; Wang, Q. K.; Mao, J. J.; Kong, X. Y. *Appl. Phys. Lett.* **2007**, *90*, 113111.
(14) (a) Liang, S.; Islam, R.; Smith, D. J.; Bennett, P. A.; O'Brien, J. R.; Taylor, B. *Appl. Phys. Lett.* **2006**, *88*, 113111. (b) He, Z. A.; Smith, D. J.; Bennett, P. A. *Phys. Rev. Lett.* **2004**, *93*, 256102. (c) Chen, S. Y.; Chen, L. J. *Appl. Phys. Lett.* **2005**, *87*, 253111. (d) Chen, S. Y.; Chen, H. C.; Chen, L. J. *Appl. Phys. Lett.* **2006**, *88*, 193114.
(15) Solberg, J. *Acta Crystallogr., Sect. A* **1978**, *34*, 684–698.
(16) (a) Rossi, G.; Kendelewicz, T.; Lindau, I.; Spicer, W. E. *J. Vac. Sci. Technol. A* **1983**, *1*, 987–990. (b) Cros, A.; Aboelfotoh, M. O.; Tu, K. N. *J. Appl. Phys.* **1990**, *67*, 3328–3336. (c) Chromik, R. R.; Neils, W. K.; Cotts, E. J. *Phase Transformations and Systems Driven Far from Equilibrium* **1998**, *481*, 581–586.
(17) (a) Daugy, E.; Mathiez, P.; Salvan, F.; Layet, J. M. *Surf. Sci.* **1985**, *154*, 267–283. (b) Mundschau, M.; Bauer, E.; Telieps, W.; Swiech, W. *J. Appl. Phys.* **1989**, *65*, 4747–4752.
(18) Banholzer, W. F.; Burrell, M. C. *Surf. Sci.* **1986**, *176*, 125–133.
(19) Corn, S. H.; Falconer, J. L.; Czanderna, A. W. *J. Vac. Sci. Technol., A* **1988**, *6*, 1012–1016.
(20) Cros, A.; Muret, P. *Mater. Sci. Rep.* **1992**, *8*, 271–367.
(21) Floquet, N.; Yilmaz, S.; Falconer, J. L. *J. Catal.* **1994**, *148*, 348–368.

(22) (a) Zilani, M. A. K.; Xu, H.; Wang, X. S.; Wee, A. T. S. *Appl. Phys. Lett.* **2006**, *88*, 023121. (b) Cheng, S. L.; Lu, S. W.; Wong, S. L.; Chang, C. C.; Chen, H. *J. Cryst. Growth* **2007**, *300*, 473–477. (c) Wi, J. S.; Lee, T. Y.; Kim, H. M.; Lee, H. S.; Nam, S. W.; Shin, I. J.; Shin, K. H.; Kim, K. B. *Adv. Mater.* **2007**, *19*, 3469. (d) Fernandez, L.; Loffler, M.; Cordon, J.; Ortega, J. E. *Appl. Phys. Lett.* **2007**, *91*, 263106.

(23) (a) Ahmadi, T. S.; Wang, Z. L.; Green, T. C.; Henglein, A.; ElSayed, M. A. *Science* **1996**, *272*, 1924–1926. (b) Alivisatos, A. P. *Science* **1996**, *271*, 933–937. (c) Kong, X. Y.; Wang, Z. L. *Nano Lett.* **2003**, *3*, 1625–1631. (d) Fan, H. J.; Werner, P.; Zacharias, M. *Small* **2006**, *2*, 700–717. (e) Xiao, Z. L.; Han, C. Y.; Kwok, W. K.; Wang, H. W.; Welp, U.; Wang, J.; Crabtree, G. W. *J. Am. Chem. Soc.* **2004**, *126*, 2316–2317.

(24) Fleury, V. *Nature* **1997**, *390*, 145–148.

(25) Zhang, Z.; Wang, S. J.; Yu, T.; Wu, T. *J. Phys. Chem. C* **2007**, *111*, 17500–17505.

(26) *ASM Handbooks Online*.

(27) Wager, R. S.; Ellis, W. C. *Appl. Phys. Lett.* **1964**, *4*, 89.

(28) Hubbard, K. J.; Schlom, D. G. *J. Mater. Res.* **1996**, *11*, 2757–2776.

(29) Glangregorio, M. M.; Losurdo, M.; Sacchetti, A.; Capezzuto, P.; Bruno, G. *J. Lumin.* **2006**, *121*, 322–326.

(30) Alessandrini, E. I.; Campbell, D. R.; Tu, K. N. *J. Appl. Phys.* **1974**, *45*, 4888.

(31) (a) Li, J. L.; Jia, J. F.; Liang, X. J.; Liu, X.; Wang, J. Z.; Xue, Q. K.; Li, Z. Q.; Tse, J. S.; Zhang, Z. Y.; Zhang, S. B. *Phys. Rev. Lett.* **2002**, *88*, 066101. (b) Pan, M. H.; Liu, H.; Wang, J. Z.; Jia, J. F.; Xue, Q. K.; Li, J. L.; Qin, S.; Mirsaidov, U. M.; Wang, X. R.; Markert, J. T.; Zhang, Z. Y.; Shih, C. K. *Nano Lett.* **2005**, *5*, 87–90.

NL8015208